Configuration of NEMO 4 with a wetting-and-drying scheme for the Bay of Fundy and the Saint John harbour

Chengzhu Xu, Rachel Horwitz, Xianmin Hu, Jérôme Chanut,
Stephanne Taylor, and Youyu Lu

Ocean and Ecosystem Sciences Division
Maritimes Region
Fisheries and Oceans Canada

Bedford Institute of Oceanography
PO Box 1006
Dartmouth, Nova Scotia
Canada B2Y 4A2

2022

Canadian Technical Report of
Hydrography and Ocean Sciences 346

Fisheries and Oceans Canada | Pêches et Océans Canada

Canada

Canadian Technical Report of Hydrography and Ocean Sciences

Technical reports contain scientific and technical information of a type that represents a contribution to existing knowledge but which is not normally found in the primary literature. The subject matter is generally related to programs and interests of the Oceans and Science sectors of Fisheries and Oceans Canada.

Technical reports may be cited as full publications. The correct citation appears above the abstract of each report. Each report is abstracted in the data base *Aquatic Sciences and Fisheries Abstracts.*

Technical reports are produced regionally but are numbered nationally. Requests for individual reports will be filled by the issuing establishment listed on the front cover and title page.

Regional and headquarters establishments of Ocean Science and Surveys ceased publication of their various report series as of December 1981. A complete listing of these publications and the last number issued under each title are published in the *Canadian Journal of Fisheries and Aquatic Sciences*, Volume 38: Index to Publications 1981. The current series began with Report Number 1 in January 1982.

Rapport technique canadien sur l'hydrographie et les sciences océaniques

Les rapports techniques contiennent des renseignements scientifiques et techniques qui constituent une contribution aux connaissances actuelles mais que l'on ne trouve pas normalement dans les revues scientifiques. Le sujet est généralement rattaché aux programmes et intérêts des secteurs des Océans et des Sciences de Pêches et Océans Canada.

Les rapports techniques peuvent être cités comme des publications à part entière. Le titre exact figure au-dessus du résumé de chaque rapport. Les rapports techniques sont résumés dans la base de données *Résumés des sciences aquatiques et halieutiques*.

Les rapports techniques sont produits à l'échelon régional, mais numérotés à l'échelon national. Les demandes de rapports seront satisfaites par l'établissement auteur dont le nom figure sur la couverture et la page de titre.

Les établissements de l’ancien secteur des Sciences et Levés océaniques dans les régions et à l'administration centrale ont cessé de publier leurs diverses séries de rapports en décembre 1981. Vous trouverez dans l'index des publications du volume 38 du *Journal canadien des sciences halieutiques et aquatiques*, la liste de ces publications ainsi que le dernier numéro paru dans chaque catégorie. La nouvelle série a commencé avec la publication du rapport numéro 1 en janvier 1982.

Canadian Technical Report of
Hydrography and Ocean Sciences 346

2022

Configuration of NEMO 4 with a wetting-and-drying scheme for the Bay of Fundy and the Saint John harbour

by

Chengzhu Xu, Rachel Horwitz, Xianmin Hu, Jérôme Chanut[1],
Stephanne Taylor, and Youyu Lu

Ocean and Ecosystem Sciences Division
Maritimes Region
Fisheries and Oceans Canada
Bedford Institute of Oceanography
PO Box 1006
Dartmouth, Nova Scotia
Canada B2Y 4A2

[1]Mercator Ocean International, 2 Avenue de l'Aérodrome de Montaudran, 31400 Toulouse, France

Cat. No. Fs 97-18/346E-PDF ISBN 978-0-660-46470-1 ISSN 1488-5417

Correct Citation for this publication:

Xu, C., Horwitz, R., Hu, X., Chanut, J., Taylor, S. and Lu, Y. 2022. Configuration of NEMO 4 with a wetting-and-drying scheme for the Bay of Fundy and the Saint John harbour. Can. Tech. Rep. Hydrogr. Ocean Sci. 346: iii + 15p.

Abstract

Xu, C., Horwitz, R., Hu, X., Chanut, J., Taylor, S. and Lu, Y. 2022. Configuration of NEMO 4 with a wetting-and-drying scheme for the Bay of Fundy and the Saint John harbour. Can. Tech. Rep. Hydrogr. Ocean Sci. 346: iii + 15p.

Version 4.0 of the Nucleus of European Modelling of the Ocean (NEMO) is applied to update the coastal ocean models for the Bay of Fundy and the Saint John harbour previously developed with version 3.6 of NEMO. Version 4.0 of NEMO enables the use of a terrain-following vertical coordinate system and a wetting-and-drying scheme, both of which are essential for accurately modelling the region where the tidal range is among the largest in the world. This report introduces some technical details regarding the model setup, including the vertical coordinates, treatment of bathymetry data, surface and lateral open boundary forcing, and model parameters. It also discusses the similarity and difference between the current configurations and the previous configurations developed with NEMO 3.6. Preliminary results of model simulations and evaluation are presented. The model's potential performance is expected to further improve as we continue to optimize the new features of the model.

Résumé

Xu, C., Horwitz, R., Hu, X., Chanut, J., Taylor, S. and Lu, Y. 2022. Configuration of NEMO 4 with a wetting-and-drying scheme for the Bay of Fundy and the Saint John harbour. Can. Tech. Rep. Hydrogr. Ocean Sci. 346: iii + 15p.

La version 4.0 du système de modélisation NEMO (Nucleus for European Modelling of the Ocean) est utilisée pour mettre à jour les modèles de représentation des eaux océaniques côtières pour la baie de Fundy et le port de Saint John précédemment élaborés avec la version 3.6 du système NEMO. La version 4.0 de NEMO permet l'utilisation d'un système de coordonnées verticales de suivi de terrain et d'un schéma de mouillage et de séchage, deux éléments essentiels pour modéliser avec précision la région où l'amplitude des marées est parmi les plus importantes au monde. Ce rapport présente certains détails techniques concernant la configuration du modèle, y compris les coordonnées verticales, le traitement des données de bathymétrie, le forçage de la surface et des limites ouvertes latérales et les paramètres du modèle. Il aborde également les similitudes et les différences entre les configurations actuelles et les configurations précédentes élaborées avec NEMO 3.6. Les résultats préliminaires des simulations et de l'évaluation du modèle sont présentés. Le rendement potentiel du modèle devrait s'améliorer davantage au fur et à mesure que nous continuons à optimiser les nouvelles fonctionnalités du modèle.

1 Introduction

The Bay of Fundy has tidal ranges that are among the largest in the world, which is a result of the near resonance of the semi-diurnal tidal forcing with the natural frequency of oscillation due to the Bay's geometry (Garrett, 1972, 1974). The tidal range reaches a maximum of around 16 m in the upper bay and about 8 m in the Saint John harbour. Near the Saint John harbour, the complexity of the ocean dynamics is further increased due to the interaction of tidal flows with freshwater discharge from the Saint John River. During high tides, the interaction leads to the generation of a sharp front near the harbour. Moreover, the tidal flows also interact with the complex geometry and bathymetry of the channel and lake system connecting the harbour and the river. In particularly, at the location known as the Reversing Falls, the flow conditions change drastically over the course of each tidal cycle (Horwitz et al., 2021).

Located in the Bay of Fundy, the port of Saint John is one of several major ports in eastern Canada. There exists significant marine traffic in the Saint John harbour, including tankers, containers and cruise ships. Given the complexity of oceanographic conditions and the existence of heavy marine traffic, hydrodynamic modelling for the Bay of Fundy and the port of Saint John has been part of the Government of Canada's Ocean Protection Plan (OPP), which aims to increase Canada's marine safety and environmental emergency response capability. In the past several years, the OPP team has developed high-resolution models for the Bay of Fundy and the Saint John harbour, for the purpose of short-term operational forecasting (Paquin et al., 2020). The models, developed based on the Nucleus of European Modelling of the Ocean (NEMO; Madec and NEMO System Team, 2016) version 3.6, are able to reasonably represent the tidal and non-tidal dynamics at port-scale resolutions. After the initial development and validation, the OPP team continues to improve these models toward operationalization.

One of the major limitations of NEMO 3.6 is the lack of a wetting-and-drying (WAD) scheme that can represent the dynamics in the inter-tidal zone (tidal flats). Due to the extremely large tidal amplitudes, extended inter-tidal zones exist in the Saint John harbour and throughout the Bay of Fundy. In the new version of the model, NEMO 4.0, a terrain-following (sigma-level) vertical coordinate system and a WAD scheme is available. In the Bay of Fundy and the Saint John harbour, both of these features are essential for accurately simulating dynamics in the inter-tidal zone. With the implementation of these features, the model has the potential to better represent the tidal dynamics over the entire domain.

In this report, we present a recent effort to develop model configurations based on NEMO version 4.0.4. The purpose of this report is to provide a reference of the technical aspects for setting up model configurations with sigma-coordinates and wetting and drying in NEMO version 4.0 and higher. Following a brief summary of the previous configurations of the model based on NEMO 3.6, we document technical details of creating configurations based on NEMO 4.0.4 in Section 2. Model evaluation based on preliminary model results is presented in Section 3, although a full evaluation is beyond the scope of this report. The ongoing and future work for model development is discussed in Section 4.

2 Model configurations

The model configurations presented by Paquin et al. (2020) consist of a three-level, one-way nesting downscaling system. The configuration on the first level of the downscaling system is referred to as BoFSS1/36. It covers the Bay of Fundy and the Scotian Shelf with a horizontal resolution of 2.5 km (nominally 1/36° in latitude–longitude), and is initialized from and forced at the open boundaries by the 1/12° Regional Ice Ocean Prediction System (RIOPS; Dupont et al., 2015). The configurations on the second and third levels are referred to as BoF500 and SJAP100, respectively, where BoF500 covers the Bay of Fundy with a horizontal resolution of 500 m, and SJAP100 covers the Saint John harbour and approach with a horizontal

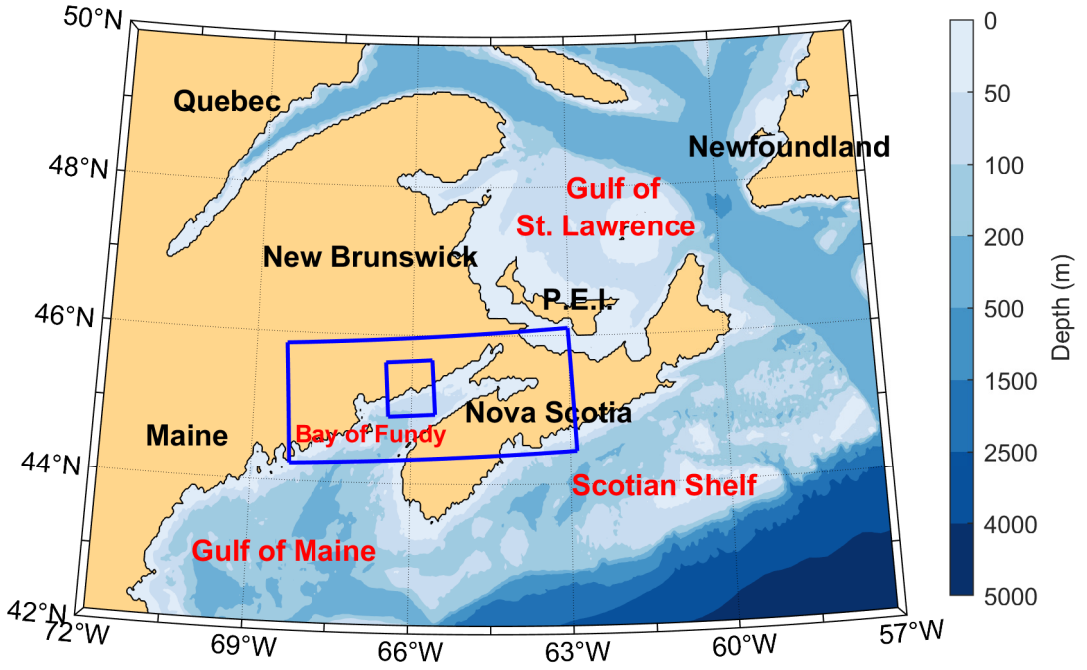

Figure 1: Bathymetry map showing the location of Bay of Fundy. The larger box indicates the BoF500 domain and the smaller box indicates the SJAP100 domain. The BoFSS1/36 domain is not shown as it is no longer part of the current version of model configurations.

resolution of 100 m (Figure 1). The horizontal grids of all three configurations are aligned with the ORCA tri-polar grids (DRAKKAR Group, 2007) to simplify the downscaling from RIOPS. In the vertical direction, a z-level coordinate system with bottom partial steps and nonlinear free surface is implemented using the variable volume level (VVL) scheme (Levier et al., 2007), which allows the stretching and compression of the thickness of vertical layers according to the changes of sea surface height (SSH).

In this work, NEMO version 4.0.4 is applied to replace NEMO 3.6 for BoF500 and SJAP100. The new version of these configurations follow the same grid-nesting approach so that the model domains and horizontal grids are the same as those reported by Paquin et al. (2020). A new version of BoFSS1/36 is not developed, since the new BoF500 takes the lateral open boundary forcing directly from the Coastal Ice-Ocean Prediction Systems for the east coast of Canada (CIOPS-E; Paquin et al., 2021, `https://eccc-msc.github.io/open-data/msc-data/nwp_ciops/readme_ciops_en/`), instead of from BoFSS1/36.

2.1 Vertical coordinates

In the new version of BoF500 and SJAP100, the sigma-level coordinate system is employed in the vertical direction (activated by `ln_sco`), which better represents the bottom boundary and is commonly used in coastal and shelf ocean modelling. The vertical levels of the sigma coordinates are stretched uniformly if h, the depth of the sea bed (specified by the bathymetry; see Section 2.3), is smaller than h_c, the critical depth (specified by `rn_hc` in the namelist), and non-uniformly otherwise. For uniform stretching, the stretching factor s for each vertical level k is given by

$$s(k) = -\frac{k-1}{n-1}, \quad k = 1, \ldots, n, \tag{1}$$

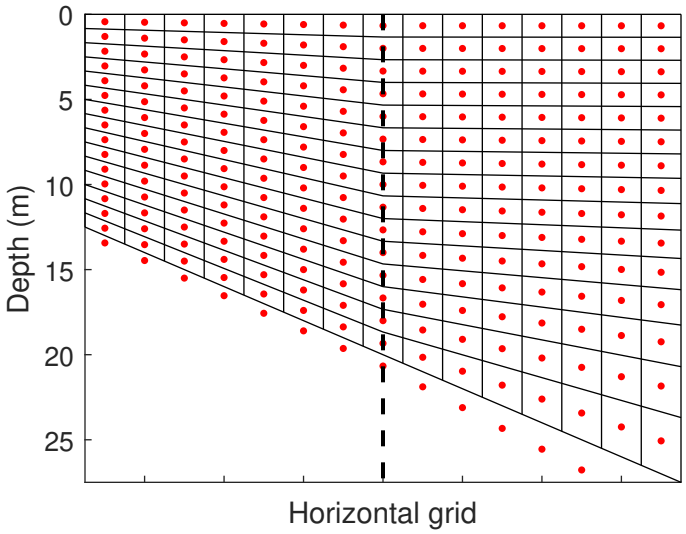

Figure 2: Schematic diagram showing the distribution of T-grid points (red dots) and cells in a terrain-following coordinate system. Dashed line separates the region of uniform stretching (left) from the region of non-uniform stretching (right). The last level of the T-grid points are below the ocean bottom. For clarity of presentation, every other level is shown.

where n is the total number of vertical levels. Here, k is ordered such that $k = 1$ is the surface level and $k = n$ is the bottom level. For non-uniform stretching, a stretching function $C(s)$ modified from that of Song and Haidvogel (1994) (enabled by setting `ln_s_sh94 = .true.` in the namelist) is used to determine the stretching factor,

$$C(s) = (1-b)\frac{\sinh(\theta s)}{\sinh(\theta)} + b\frac{\tanh[\theta(s+0.5)] - \tanh(0.5\theta)}{2\tanh(0.5\theta)}, \tag{2}$$

where θ is the surface control parameter (`rn_theta` in the namelist), b is the bottom control parameter (`rn_bb` in the namelist), and s is defined in Equation (1).

In NEMO 4, spatial discretization is pre-processed through the external tool, `DOMAINcfg`, before the simulation starts. It takes `coordinates.nc` and `bathy_meter.nc` as input data for the horizontal coordinates and the bathymetry, respectively, and reads configuration parameters for horizontal and vertical discretization from its own namelist. For the sigma-level coordinate system described above, the depths of vertical velocity (W) and tracer (T) grids, `gdepw_0` and `gdept_0`, are given by

$$\texttt{gdepw\_0}(i,j,k) = \begin{cases} h(i,j)s(k), & \text{if } h(i,j) < h_c, \\ [h(i,j) - h_c]C(s(k)) + h_c s(k), & \text{if } h(i,j) \geq h_c, \end{cases} \tag{3}$$

and

$$\texttt{gdept\_0}(i,j,k) = \begin{cases} h(i,j)s(k+0.5), & \text{if } h(i,j) < h_c, \\ [h(i,j) - h_c]C(s(k+0.5)) + h_c s(k+0.5), & \text{if } h(i,j) \geq h_c, \end{cases} \tag{4}$$

respectively. The last level of the T-grid is below the ocean bottom, and is permanently masked as land. In the current configurations, 31 vertical levels are used, and the following values are adopted for specifying the stretching of the vertical coordinates:

```
rn_hc       =   20.0    !  critical depth for transition to stretched coordinates
rn_rmax     =    1.0    !  maximum cut-off r-value allowed (0<r_max<1)
rn_theta    =    6.0    !  sigma 6.0    !  surface control parameter (0<=theta<=20)
rn_bb       =    0.0    !  stretching with SH94 s-sigma
```

A schematic diagram of the vertical coordinate system defined with these parameters is shown in Figure 2. As shown in the figure, in the region of non-uniform stretching the distribution of the vertical levels is surface intensified, which is optimized for simulating near-surface processes as in the previous model configurations. For future work, different stretching of the vertical coordinates should be tested.

The grid variables generated by `DOMAINcfg` are saved in `domain_cfg.nc`. When the simulation starts, these variables are loaded into the memory by setting `ln_read_cfg = .true.` and `cn_domcfg = "domain_cfg"` in the namelist. As in the previous configurations, the VVL scheme (Levier et al., 2007) is adopted during the simulation and the vertical coordinates are stretched and compressed according to the changes of SSH.

2.2 Wetting and drying

Previous studies (e.g. Greenberg et al., 2005; Dupont et al., 2005) have shown that enabling WAD is important for modelling the upper Bay of Fundy. In the new version developed under NEMO 4.0, WAD is implemented using the directional limiter (activated by `ln_wd_dl`) based on the scheme developed by Warner et al. (2013). In the model, a tracer cell is considered dry if its instantaneous water depth (i.e., SSH plus bottom depth) is equal to or less than a predetermined value, specified by `rn_wdmin1` in the namelist. In the current configurations, `rn_wdmin1` is set to 0.3 m. The WAD scheme monitors the water depth and determines the flow direction on each barotropic sub-step. When a cell becomes dry, surface fluxes for this cell are switched off to prevent freezing and boiling and, with the directional limiter, outflow of the water from the dry cell is not allowed (while inflow is still allowed) to prevent it from drying out further. This is achieved by setting the velocity across the face of the dry cell to zero if the flux is from the cell (while flux to the cell remain unaffected). With this treatment, water depth of the dry cell remains positive. On each baroclinic time step, the velocity at the tracer cell faces are carefully calculated to be equal to its mean value during the barotropic sub-steps. Hence, the WAD scheme is able to conserve tracers in the dry cell. Moreover, for dry cells with water depth less than `rn_wdmin1`, fluctuation of water level is still allowed, so that the total volume of the entire system is conserved.

2.3 Bathymetry

The bathymetry and coastline data used in the model are provided by the Canadian Hydrographic Service. Because of the extremely large tidal range and the lack of a wetting-and-drying scheme in NEMO 3.6, the bathymetry of the upper Bay of Fundy was adjusted in the previous version to ensure that no grid cells in the ocean domain ever dried. Some regions were deepened so that the water depth would not approach zero at low tide, and other regions were masked as land points, including most of the inter-tidal zone. In this NEMO4 version, the model bathymetry is based on the same dataset as in Paquin et al. (2020), but now the bathymetry is no longer modified to avoid wetting and drying. Instead, smoothing of the bathymetry is needed in order to reduce the horizontal pressure gradient error, which commonly occurs over steep slopes in the sigma-level coordinate system (Haney, 1991; Beckmann and Haidvogel, 1993; Song, 1998; Mellor et al., 2002; Ezer and Mellor, 2004). Bathymetry smoothing can be done in several ways. For example, a maximum slope factor can be imposed into the bathymetry data using the method described in Sikirić et al. (2009). Letting h denote the depth of the ocean bottom, the slope factor rx_0 over two adjacent cells e and e' is defined by

$$rx_0(h; e, e') = \frac{|h(e) - h(e')|}{h(e) + h(e')}. \tag{5}$$

In the current model configurations, the maximum slope factor is set to 0.2. In the BoF500 domain, bathymetry smoothing is not practical near Reversing Falls due to the complex river geometry and the model's coarse resolution relative to the river width. Instead, the Saint John River is set to 20 m depth, with a single cell of 12 m depth at Reversing Falls.

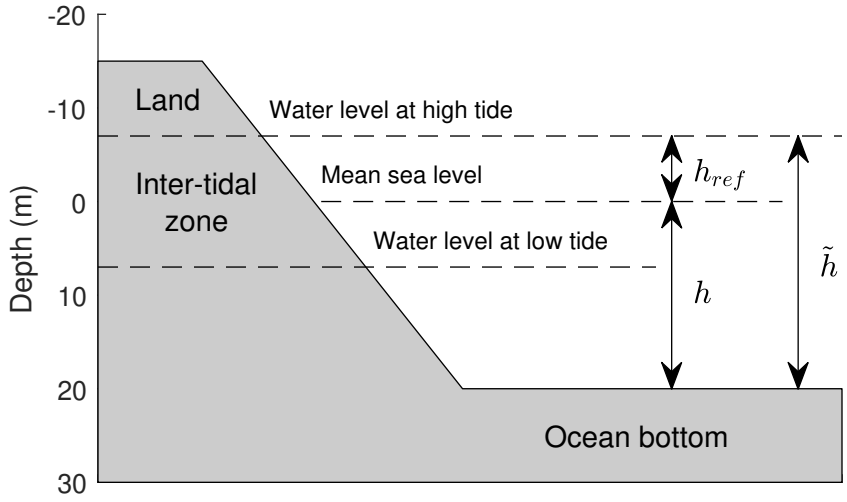

Figure 3: Schematic diagram showing the original bathymetry h (referenced to the mean sea level), the reference depth $h_{\rm ref}$, and the input bathymetry $\tilde{h}$ (referenced to the water level at high tide).

With the implementation of the WAD scheme, topography above the mean sea level (negative bathymetry) should be incorporated into the bathymetry data in order to correctly simulate the dynamics in the inter-tidal zone. However, in NEMO 4.0, the `DOMAINcfg` tool requires the input bathymetry from `bathy_meter.nc` to be positive for all grid cells in the ocean domain, including those in the inter-tidal zone. To meet this constraint, the original bathymetry, h, is modified by adding a positive reference depth, $h_{\rm ref}$, so that the input bathymetry, $\tilde{h}$, is given by

$$\tilde{h} = h + h_{\rm ref}. \tag{6}$$

As illustrated in Figure 3, $h_{\rm ref}$ should be large enough to allow $\tilde{h}$ to be positive for all grid cells in the inter-tidal zone. `DOMAINcfg` will then determine the layer thickness for any grid cells with positive $\tilde{h}$, whereas those with zero or negative $\tilde{h}$ will be masked as land.

The largest negative value in our bathymetry data is -5 m, so we set $h_{\rm ref} = 5$ m in the current configurations. In the SJAP100 domain, the maximum tidal amplitude is about 3 m. Setting $h_{\rm ref} = 5$ m allows `DOMAINcfg` to create a grid system with an ocean domain that covers all inter-tidal zones. In the BoF500 domain, the maximum tidal amplitude is about 6 m. Setting $h_{\rm ref} = 5$ m leads to a few (less than 10) grid cells in the inter-tidal zones in the upper Bay of Fundy to be masked as land. If a bathymetric data product were available that included larger vertical relief in the upper Bay of Fundy, then the entire intertidal zone can be simulated by setting $h_{\rm ref}$ to be larger than 6 m for BoF500.

When `DOMAINcfg` generates a vertical grid based on the artificially deepened $\tilde{h}$, the vertical coordinates (`gdep*`) and layer thickness (`e3*`) saved in the output file, `domain_cfg.nc`, are also based on $\tilde{h}$ (e.g., in Equations (3) and (4), h is replaced by $\tilde{h}$). During the simulation, the reference depth must be removed before the VVL scheme is applied, so that the actual water depth remains as SSH $+ h$. In NEMO 4, this is done by subtracting the reference depth from the initial and boundary SSH forcing. The reference depth is specified by the parameter `rn_wd_ref_depth`, which must be added to `domain_cfg.nc` manually by, e.g.,

```
ncap2 -4 -A -s "rn_wd_ref_depth=5" domain_cfg.nc domain_cfg.nc
```

With this step, the initial and boundary SSH forcing is consistent with the SSH inside the model domain, and the VVL scheme essentially scales the vertical levels (`gdep*`) and layer thickness (`e3*`) by the factor $(\text{SSH} + h)/\tilde{h}$, instead of $(\text{SSH} + \tilde{h})/\tilde{h}$. Theoretically, this scaling will lead to zero or negative layer thickness when SSH $\leq -h$ (i.e., when a tracer cell becomes "dry"), as expected in the inter-tidal zones. In practice,

however, the water depth of a tracer cell is supposed to remain positive at all times, because the WAD scheme will prevent the cell from drying out further if the water depth is below the predetermined minimum value, `rn_wdmin1`; see Section 2.2. Hence, numerical instability due to zero or negative layer thickness is avoided during the simulation.

2.4 Model initialization

In NEMO 4.0, the temperature and salinity fields can be initialized from external data by setting `ln_tsd_init = .true.`. However, the velocity or SSH fields cannot be initialized from external data. Given the large tidal amplitude in the Bay of Fundy, this would cause numerical instabilities at the open boundaries. There are two ways to resolve this problem. The SJAP100 configuration is initialized with zero velocity and SSH. The tide ramp was turned on (`ln_tide_ramp = .true.`) for the first 7 days (`rdttideramp = 7.0`) to prevent the model from crashing due to large tidal amplitude at the open boundaries. The BoF500 configuration is initialized with velocity and SSH fields from external data by converting them into the format of a restarting file. The model is then configured to "restart" from this restarting file instead.

2.5 Surface boundary conditions

Forcing at the sea surface remains unchanged from the previous version developed under NEMO 3.6. The forcing includes hourly 10-m winds, 2-m air temperature and specific humidity, precipitation and surface incoming longwave and shortwave radiation from the 2.5-km High-Resolution Deterministic Prediction System (HRDPS; Milbrandt et al., 2016). The sea surface momentum flux, sensible and latent heat fluxes and the rate of evaporation are computed using the bulk formulae of the Coordinated Ocean-ice Reference Experiments (CORE; Large and Yeager, 2004).

2.6 Lateral open boundary conditions

For the new version developed under NEMO 4.0, lateral open boundary conditions are implemented following a procedure similar to that in the previous version under NEMO 3.6, with the exception that the new BoF500 is forced by CIOPS-E instead of BoFSS1/36. Forcing variables for the lateral open boundaries include sea surface height (SSH) and three-dimensional fields of horizontal velocities, temperature, and salinity. For baroclinic velocities, temperature, and salinity, a flow relaxation scheme (Engedahl, 1995) is applied to a 10-grid-point wide relaxation zone inside the lateral boundaries. For SSH and barotropic (depth-averaged) velocities normal to the boundaries, the radiation scheme of Flather (1976) is applied. The barotropic velocities tangential to the boundaries are set to be equal to the values from the outer domain.

In the new version of BoF500, SSH and barotropic velocities at the lateral open boundaries from CIOPS-E are de-tided, because tidal solutions from CIOPS-E are not sufficiently accurate in the Bay of Fundy. Instead, solutions of five main tidal constituents (M2, N2, S2, K1 and O1) from WebTide (Dupont et al., 2005) are used as the tidal boundary forcing. For the new SJAP100, boundary conditions are currently obtained from the output of the previous version of BoF500. Because its output has an hourly frequency which is not high enough to accurately resolve the tidal signals, SSH and barotropic velocities are also de-tided. The tidal signals are then introduced by adding the five tidal constituents (M2, N2, S2, K1 and O1) reconstructed from harmonic analysis of the hourly output of BoF500. In the near future, higher frequency output of the new version of BoF500 will be used when it is fully tuned and validated.

In this downscaling system, spatial interpolation is required to take input data from the coarser parent grid onto the finer child grid. In the sigma-level coordinate system, the vertical grid varies spatially. The three-dimensional variables specifying the depths of the vertical levels, `gdep*`, and the corresponding layer

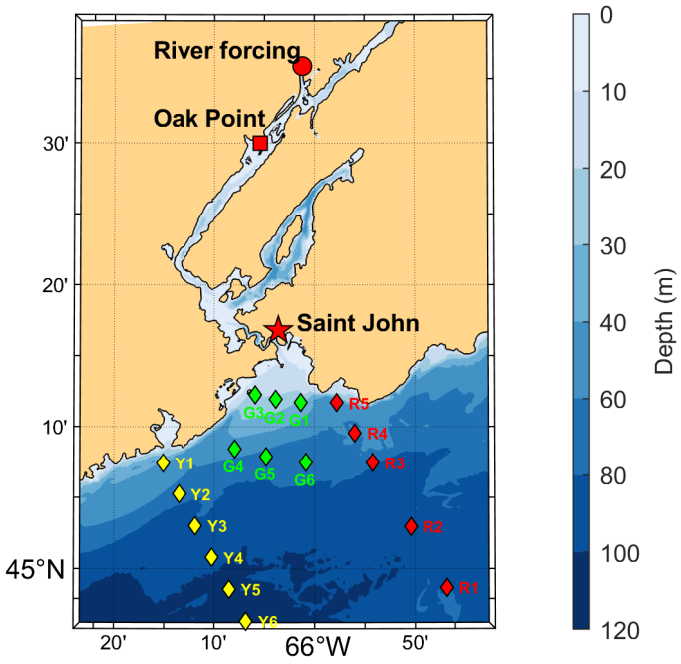

Figure 4: Bathymetry map of the SJAP100 domain showing the locations of Saint John (red pentagram), Oak Point station (red square), and where river forcing is imposed (red dot). The red, green and yellow diamonds indicate locations at which model evaluation is performed; see Section 3.

thickness, `e3*`, are available in the `mesh_mask` files. When interpolating onto a child grid with a reference depth, the layer thickness of the child grid must be scaled by $h/\tilde{h}$ for the reason described in Section 2.3, so that the total water depths between the two grids are consistent.

To avoid complications when interpolating from a parent grid that does not support WAD, we avoid WAD near open boundaries in the child grid by deepening those grid cells, so that the total water depths in the parent and child grids are consistent. Otherwise, negative water depth could be imposed onto the child grid, which causes error in the current version of NEMO 4.0.

2.7 River boundary conditions

In both the previous and new versions of BoF500 and SJAP100, runoff from the Saint John River is imposed as a boundary forcing at a location that is far enough upstream where the tidal amplitude is small and the salinity is close to zero (indicated by the red dot in Figure 4). The river boundary forcing includes water level observed at the Oak Point station and water temperature measured at the Tracey Mills station. The water level reported at the Oak Point station is referenced to Canadian Geodetic Vertical Datum of 1928 (CGVD28), which is the same as that used in SJAP100 and BoF500. Thus, the reported water level at Oak Point is directly applied as the SSH for river forcing.

2.8 Model parameters

In NEMO, a time-splitting scheme is applied for the internal (baroclinic) and external (barotropic) modes. In the new version developed under NEMO 4.0, the lengths of each model time step for the internal (external)

mode are set to be 30 s (1 s) and 6 s (0.6 s) for BoF500 and SJAP100, respectively. The momentum advection follows the standard second-order vector form scheme (`ln_dynadv_vec`), while the horizontal tracer advection follows a second-order flux corrected transport scheme (`ln_traadv_fct`). In the vertical direction, the newly available adaptive-implicit vertical advection scheme (`ln_zad_Aimp`; Shchepetkin, 2015) is adopted, which improves the numerical stability. The horizontal mixing is applied along the sigma levels of the current configurations and is parameterized using the Laplacian diffusion scheme for both momentum (`ln_dynldf_lap`) and tracer (`ln_traldf_lap`). Following Smagorinsky (1993), the three-dimensional, time-varying viscosity is estimated from the local deformation rate based on the horizontal shear and tension. For numerical stability, the upper and lower limits are set to

$$\frac{C_{\max}(\Delta x)^2}{8\Delta t} \quad \text{and} \quad 0.5 C_{\min} \Delta x |U|, \tag{7}$$

respectively, where Δx is the local grid spacing, U is the local velocity, and Δt is the length of model time step. The two constants, $C_{\max}$ (`rn_maxfac`) and $C_{\min}$ (`rn_minfac`), are set to 0.5 and 0.16, respectively. The tracer diffusivity is set to be a function of local grid spacing and velocity magnitude,

$$\frac{1}{12} \Delta x |U|. \tag{8}$$

The vertical mixing is calculated using the $k - \epsilon$ configuration of the generic length scale (GLS) turbulence closure (`ln_zdfgls`; Umlauf and Burchard, 2003, 2005), with the background vertical eddy viscosity (`rn_avm0`) and diffusivity (`rn_avt0`) set to 1.2×10^{-4} m^2/s and 1.2×10^{-5} m^2/s, respectively.

The bottom drag coefficient is computed following the logarithmic layer formula (`ln_loglayer`),

$$C_D = \left(\frac{\kappa}{\ln(0.5 z_b / z_0)} \right)^2, \tag{9}$$

where κ is the von-Karman constant ($\kappa = 0.4$ is used in NEMO), z_b is the thickness of the bottom layer, and z_0 is the roughness length scale specified by `rn_z0` in the namelist. In both BoF500 and SJAP100, z_0 is set to 0.003 m, while the minimum drag coefficient (`rn_Cd0`) set to 0.004. It can be shown that C_D determined from Equation (9) is less than 0.004 if $z_b > 3.35$ m. Given the vertical coordinates that are specified as described in Section 2.1, this means that $C_D < 0.004$ if the water depth is greater than approximately 38.48 m. This parameterization thus implies that within the BoF500 domain, the minimum drag coefficient 0.004 is imposed over the majority of the open waters where the layer thickness is large and the logarithmic layers are not resolved, while drag coefficient determined by Equation (9) is imposed only over the coastal regions, the Saint John River, and part of the upper Bay of Fundy.

3 Preliminary model results and evaluation

In this section, model evaluation is performed based on the preliminary model results. However, because the purpose of this report is limited to the technical aspects of setting up model configurations with sigma-coordinates and wetting and drying in NEMO 4.0.4, a full evaluation is beyond the scope of this report. Given that the current configurations are still under development and that further improvement is expected in the near future, model evaluation presented here should not be interpreted as the model's potential performance. In particular, comparison of the current version with the previous version developed under NEMO 3.6 is not given, as differences in the model setup, e.g., bathymetry adjustment, could be too significant between the two versions for a fair comparison.

3.1 Temperature and salinity

For the purpose of model validation, test runs of BoF500 and SJAP100 have been performed for a 90-day period starting from March 1, 2016. During this time period, a few CTD data are available within the

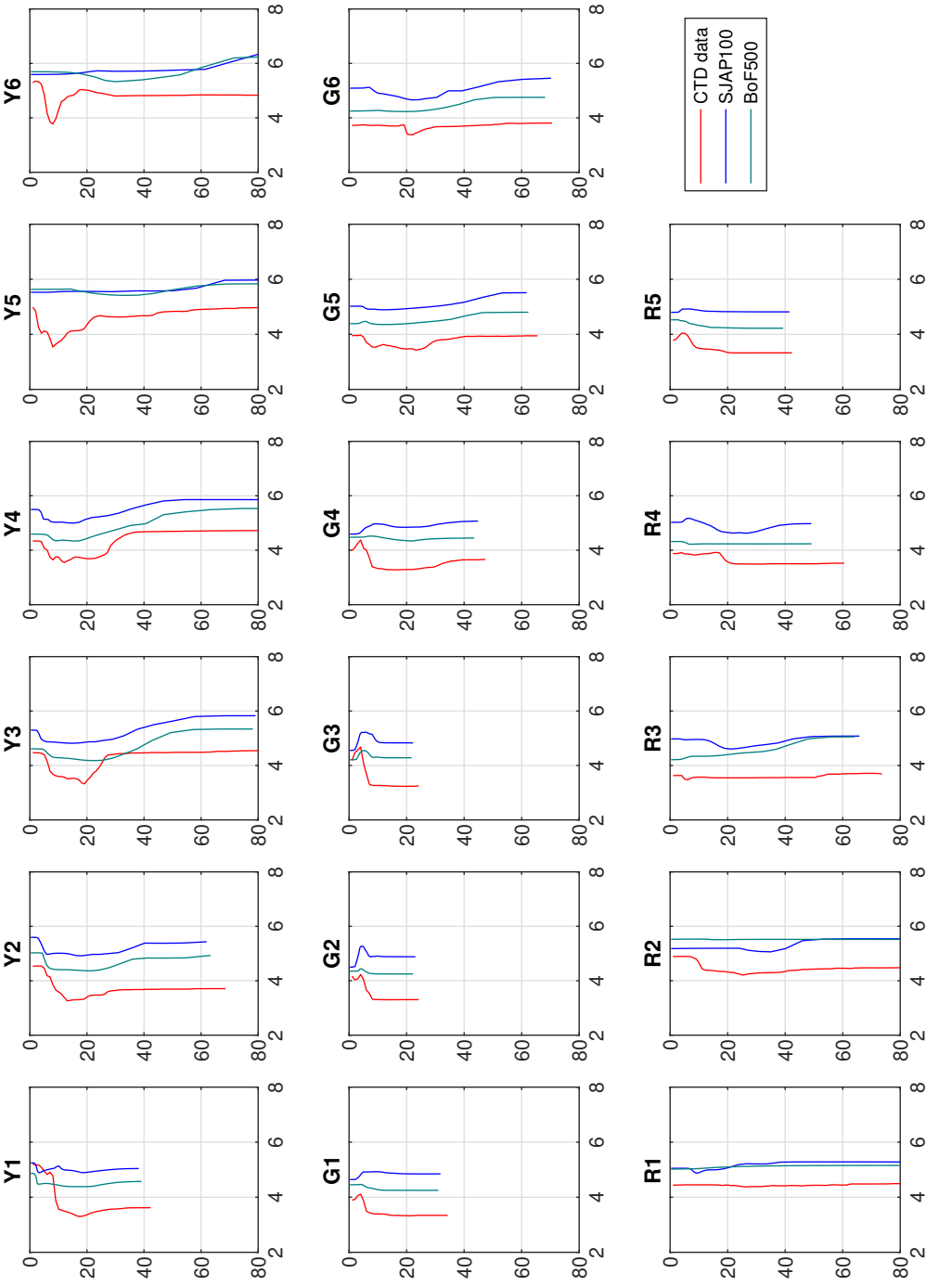

Figure 5: Comparison of temperature profiles at locations indicated in Figure 4 between observation (red), SJAP100 (blue) and BoF500 (green).

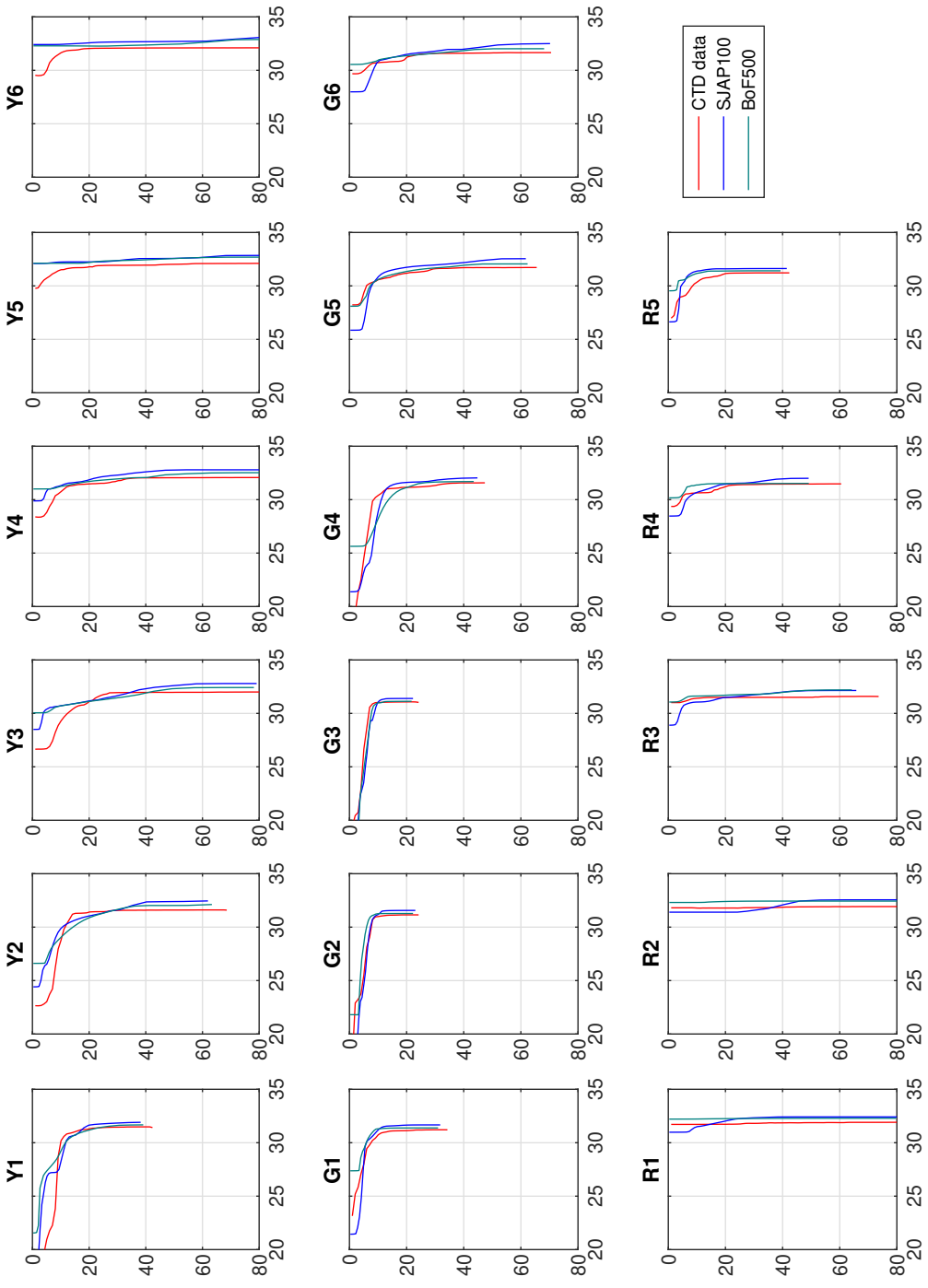

Figure 6: Comparison of salinity profiles at locations indicated in Figure 4 between observation (red), SJAP100 (blue) and BoF500 (green).

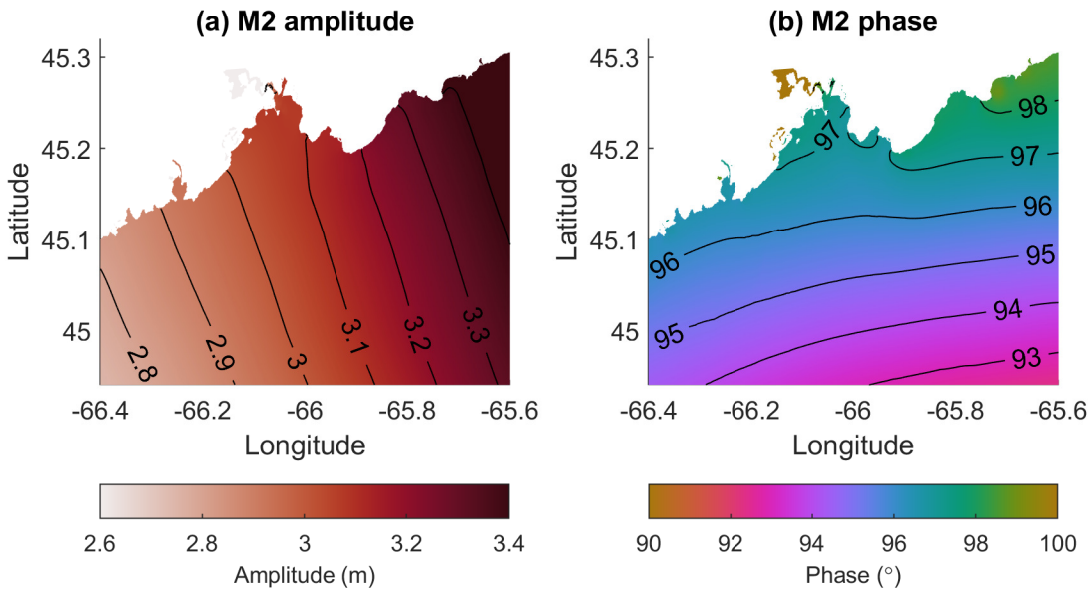

Figure 7: M2 amplitude and phase of SSH between March 12, 2016 and April 25, 2016 in the SJAP100 domain, excluding the Saint John River.

model domain. To evaluate the performance of both configurations, we compare the model results with 17 CTD casts inside the SJAP100 domain, as indicated by the red, yellow and green diamonds in Figure 4. These CTD data were collected on April 18, 2016 and April 19, 2016. The comparison of temperature and salinity between the model results and the CTD data are shown in Figures 5 and 6, respectively. Figure 5 shows that the model temperature (of both configurations) is warmer than the observed temperature of approximately 1° C almost everywhere. This temperature bias of the model occurs because CIOPS-E, which forces the current configurations from the lateral open boundaries, also over-estimates the temperature (Paquin et al., 2021). Figure 6 shows that both model configurations are able to capture the observed salinity correctly, especially in the lower layer, though there are some differences in the upper layer in some locations. Accurately modelling the upper layer salinity is difficult because the location of the fresh water front formed due to the interaction of tidal current and river plume can affect the upper layer salinity significantly. Nevertheless, the comparison shows that both configurations are able to capture the salinity stratification, in particular the depth of the halocline, reasonably accurately.

3.2 Tidal amplitude and phase

To evaluate the model's ability to simulate tides near the Saint John harbour, harmonic analysis using the `t_tide` package (Pawlowicz et al., 2002) has been performed for the SSH of the SJAP100 configuration (excluding the Saint John River) between March 12, 2016 and April 25, 2016. The amplitude and phase of the M2 tide, which is the dominant constituent in this region, are shown in Figure 7. Within this area, there exists a tide gauge[2] located on the dock of the Saint John ferry terminal near the Saint John harbour. The modelled M2 amplitude and phase at the Saint John station are 3.052 m and 97.44°, while the observed M2 amplitude and phase are 3.062 m and 96.92°. The comparison suggests a good agreement between the model and the observation, with a difference of less than 1% for both M2 amplitude and phase.

[2] `https://www.qc.dfo-mpo.gc.ca/tides/en/stations/00065`

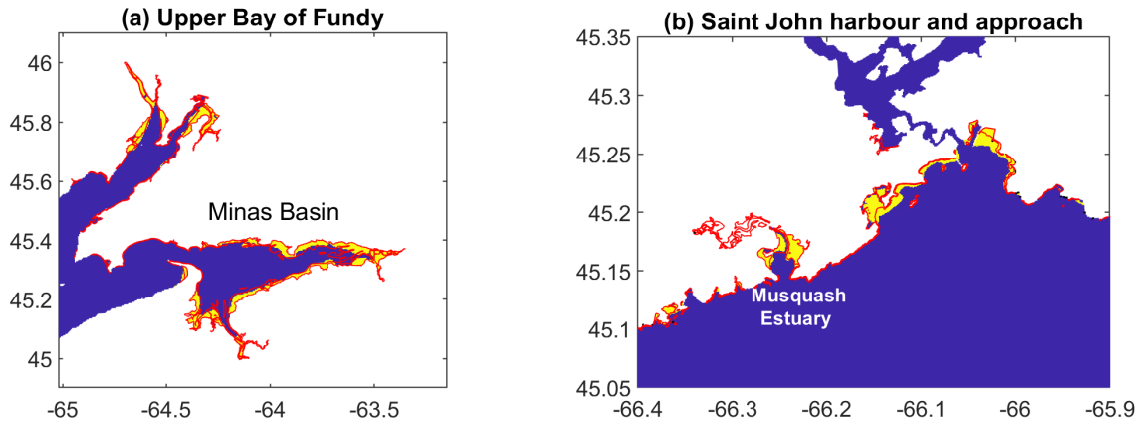

Figure 8: Map of inter-tidal zones in (a) Minas Basin and upper Bay of Fundy, and (b) Saint John harbour and approach. The area masked in yellow indicates inter-tidal zone from model output. The area enclosed by red contours indicates inter-tidal zone from CanVec data.

3.3 Wetting and drying

To evaluate the model performance on wetting and drying, Figure 8 shows a qualitative comparison of modelled inter-tidal zones and those obtained from the CanVec Data Series[3]. In the figure, the modelled inter-tidal zone is defined as any area that becomes dry between March 15, 2016 to May 15, 2016. For areas shown in the figure, the majority of the inter-tidal zones from the two data sets overlap each other, in particular the tidal flats in the Minas Basin in Panel (a) and those near the Musquash Estuary in Panel (b). This implies that the WAD scheme is performing as expected given the limited bathymetry and topography data of the inter-tidal zone currently available.

4 Ongoing and future work

4.1 Model improvement

The performance of the model can be further improved in several ways. In order to take full advantage of the WAD scheme, it is important to obtain high quality bathymetry and topography data along the coastline, so that the dynamics in the inter-tidal zone can be accurately represented. For the BoF500 domain, with a bathymetric data product that includes a vertical relief of at least 6 m above the mean sea level in the upper Bay of Fundy, the entire inter-tidal zone can be simulated by setting the reference depth larger than the expected highest water level. For the SJAP100 domain, the existing bathymetry data lacks information for some shallow coastal lagoons, and high resolution bathymetry data of the inter-tidal zone could also help to improve the model performance in those areas.

In the current version of model configurations, the sigma-level coordinate system is implemented in a way such that distribution of the vertical levels is surface intensified. This arrangement is optimized for simulating near-surface processes as in the previous model configurations. For future work, different stretching of the vertical coordinates should be tested. In particular, increasing the resolution of the vertical coordinate system near the bottom would allow the model to better represent dynamics occurring in the bottom boundary layer. Additionally, a different transformation could be tested, such as that developed by Shchepetkin and McWilliams (2005).

[3] https://open.canada.ca/data/en/dataset/8ba2aa2a-7bb9-4448-b4d7-f164409fe056

For future work, tuning of bottom drag coefficient is also needed to improve the model's accuracy of simulating bottom friction and tidal propagation. As discussed in Section 2.8, in the current configurations, variable bottom drag coefficient is only imposed over shallow coastal areas, while the bottom drag coefficient for the majority of the open ocean is set to 0.004 where the total water depth is larger than 38.48 m. In the future, variable bottom drag coefficient should also be tested in the open ocean by, e.g., imposing the canonical value of 0.0025 as the minimum drag coefficient.

4.2 Passive tracers

NEMO includes a TOP module to simulate the distribution and movement of environment variables (e.g., pollutants) as passive tracers. To activate the TOP module, the model needs to be recompiled with `key_top`. One way to initialize the tracer field is to modify `trcini_my_trc.F90`. For example, the following code sets the initial tracer field to 1 in the Saint John river and 0 everywhere else in SJAP100.

```
INTEGER :: ji, jj

IF( .NOT. ln_rsttr ) THEN
  trn(:,:,:,jp_myt0:jp_myt1) = 0._wp

  DO ji = mi0(200), mi1(600)
    DO jj = mj0(460), mj1(1009)
      trn(ji,jj,:,jp_myt0:jp_myt1) = 1._wp
    END DO
  END DO
END IF
```

To include the pre-defined tracer field in the simulation, the model should be run with `namelist_top_ref` and `namelist_top_cfg`, which should contain the following configurations,

```
jp_bgc        =  1
ln_my_trc     =  .true.
sn_tracer(1)  =  'TRC01'  , 'Tracer  Concentration                ',   ' - '    ,   .false.
```

To include the tracer field in the model output, the file `field_def_nemo-pisces.xml` is needed and the line

```
<field_definition src="./field_def_nemo-pisces.xml"/>
```

should be added to `iodef.xml`.

When testing passive tracers with the WAD scheme turned on, we found that the tracer concentration is not conserved along the edge of the dry cells. This does not happen for active tracers (temperature and salinity) since the algorithm of the WAD scheme is designed specifically to conserve these quantities (see Section 2.2 and also the NEMO Book). It is likely that the source code has not been updated to conserve passive tracers in a similar manner. This requires further investigation.

Acknowledgement

This work is supported by the Ocean Protection Plan of Government of Canada, and is greatly benefited from the previous work in model development based on NEMO 3.6. The authors thank Drs Yongsheng Wu and Michael Dunphy for their constructive reviews that helped to improve the original manuscript.

REFERENCES

Beckmann, A. and Haidvogel, D. B. (1993). Numerical simulation of flow around a tall isolated seamount. Part I: Problem formulation and model accuracy. *Journal of Physical Oceanography*, 23:1736–1753.

DRAKKAR Group (2007). Eddy-permitting ocean circulation hindcasts of past decades. *CLIVAR Exchanges*, 12:8–10.

Dupont, F., Hannah, C. G., and Greenberg, D. (2005). Modelling the sea level of the upper Bay of Fundy. *Atmosphere–Ocean*, 43:33–47.

Dupont, F., Higginson, S., Bourdallé-Badie, R., Lu, Y., Roy, F., Smith, G., Lemieux, J. F., Garric, G., and Davidson, F. (2015). A high-resolution ocean and sea-ice modelling system for the Arctic and North Atlantic oceans. *Geoscientific Model Development*, 8:1577–1594.

Engedahl, H. (1995). Use of the flow relaxation scheme in a three-dimensional baroclinic ocean model with realistic topography. *Tellus A*, 47:365–382.

Ezer, T. and Mellor, G. L. (2004). A generalized coordinate ocean model and a comparison of the bottom boundary layer dynamics in terrain-following and in z-level grids. *Ocean Modelling*, 6:379–403.

Flather, R. A. (1976). A tidal model of the northwest European continental shelf. *Mémoires de la Société royale des sciences de Liège*, 10:141–164.

Garrett, C. (1972). Tidal resonance in the Bay of Fundy and Gulf of Maine. *Nature*, 238:441–443.

Garrett, C. (1974). Normal modes of the Bay of Fundy and Gulf of Maine. *Canadian Journal of Earth Sciences*, 11:549–556.

Greenberg, D., Shore, J. A., Page, F. H., and Dowd, M. (2005). A finite element circulation model for embayments with drying intertidal areas and its application to the Quoddy region of the Bay of Fundy. *Ocean Modelling*, 10:211–231.

Haney, R. L. (1991). On the pressure gradient force over steep topography in sigma coordinate ocean models. *Journal of Physical Oceanography*, 21:610–619.

Horwitz, R. M., Taylor, S., Lu, Y., Paquin, J.-P. andSchillinger, D., and Greenberg, D. A. (2021). Rapid reduction of tidal amplitude due to form drag in a narrow channel. *Continental Shelf Research*, 213:104299.

Large, W. G. and Yeager, S. G. (2004). Diurnal to decadal global forcing for ocean and sea-ice models: the datasets and flux climatologies. Technical report, National Center for Atmospheric Research. NCAR Technical Note TN–460+STR.

Levier, B., Tréguier, A.-M., Madec, G., and Garnier, V. (2007). *Free surface and variable volume in the NEMO code.*

Madec, G. and NEMO System Team (2016). *NEMO Ocean Engine.*

Mellor, G. L., Hakkinen, S., Ezer, T., and Patchen, R. (2002). A generalization of a sigma coordinate ocean model and an intercomparison of model vertical grids. In Pinardi, N. and Woods, J. D., editors, *Ocean Forecasting: Conceptual Basis and Applications*, pages 55–72. Springer.

Milbrandt, J. A., Bélair, S., Faucher, M., Vallée, M., Carrera, M., and Glazer, A. (2016). The pan-Canadian high resolution (2.5 km) deterministic prediction system. *Weather Forecast*, 31:1791–1816.

Paquin, J.-P., Lu, Y., Taylor, S., Blanken, H. Marcotte, G., Hu, X., Zhai, L., Higginson, S., Nudds, S., Chanut, J., Smith, G. C., Bernier, N., and Dupont, F. (2020). High-resolution modelling of a coastal harbour in the presence of strong tides and significant river runoff. *Ocean Dynamics*, 70:365–385.

Paquin, J.-P., MacDermid, S., and Dupont, F. (2021). Coastal Ice Ocean Prediction System for the East Coast of Canada (CIOPS-E). Update from version 1.5.0 to 2.0.0. Technical report, Environmental and Climate Change Canada. Canadian Centre for Meteorological and Environmental Prediction Technical Note.

Pawlowicz, R., Beardsley, B., and Lentz, S. (2002). Classical tidal harmonic analysis including error estimates in MATLAB using `T_TIDE`. *Computers and Geosciences*, 28:929–937.

Shchepetkin, A. F. (2015). An adaptive, Courant-number-dependent implicit scheme for vertical advection in oceanic modeling. *Ocean Modelling*, 91:38–69.

Shchepetkin, A. F. and McWilliams, J. C. (2005). The regional oceanic modeling system (ROMS): a split-explicit, free-surface, topography-following-coordinate oceanic model. *Ocean Modelling*, 9:347–404.

Sikirić, M. D., Janeković, I., and Kuzmić, M. (2009). A new approach to bathymetry smoothing in sigma-coordinate ocean models. *Ocean Modelling*, 29:128–136.

Smagorinsky, J. (1993). Some historical remarks on the use of nonlinear viscosities. In *Large Eddy Simulation of Complex Engineering and Geophysical Flows*, volume 1, pages 69–106. Cambridge University Press.

Song, Y. (1998). A general pressure gradient formulation for ocean models. Part I: scheme design and diagnostic analysis. *Monthly Weather Review*, 126:3213–3230.

Song, Y. and Haidvogel, D. (1994). A semi-implicit ocean circulation model using a generalized topography-following coordinate system. *Journal of Computational Physics*, 115:228–244.

Umlauf, L. and Burchard, H. (2003). A generic length-scale equation for geophysical turbulence models. *Journal of Marine Research*, 61:235–265.

Umlauf, L. and Burchard, H. (2005). Second-order turbulence closure models for geophysical boundary layers. A review of recent work. *Continental Shelf Research*, 25:795–827.

Warner, J. C., Defne, Z., Haas, K., and Arango, H. G. (2013). A wetting and drying scheme for ROMS. *Computers and Geosciences*, 58:54–61.